ELSEVIER

Applied Surface Science 149 (1999) 193–197

applied surface science

Impurity–vacancy defects in implanted float-zone and Czochralski-Si

Jun Xu [a,*], A.P. Mills Jr. [b], Ryoichi Suzuki [c], E.G. Roth [a], O.W. Holland [a]

[a] *Oak Ridge National Laboratory, P.O. Box 2008, Oak Ridge, TN 37831, USA*
[b] *Bell Laboratories, Lucent Technologies, 600 Mountain Avenue, Murray Hill, NJ 07974, USA*
[c] *Electrotechnical Laboratory, 1-1-4 Umezono, Tsukuba, Ibaraki 305, Japan*

Abstract

The dual implantation method developed for defect engineering [O.W. Holland, L. Xie, B. Nelson, D.S. Zhou, J. Electron. Mater. 25 (1996) 99] uses an amorphizing implant in conjunction with high energy Si^+-ion implantation to inject vacancies. Following annealing of the implanted samples for 20 min at 600°C and at 800°C, the amorphous layer recrystallizes by solid-phase epitaxial growth (SPEG), and the unwanted interstitials are consumed by recombination with vacancies. Doppler broadening of annihilation radiation and beam positron lifetime measurements reveal that there are residual divacancy–impurity complexes formed in the SPEG layer. Since the effect is nearly identical in both float-zone and Czochralski-Si, the source of the impurities is not likely to be residual oxygen in the unimplanted crystals.

Keywords: Defect engineering; Impurity; Implantation

1. Introduction

Ion implantation is a useful technique for producing shallow electrical junctions in semiconductor devices. However, the implantation process also produces many defects (e.g., interstitials and vacancies). These defects can contribute to substantial broadening of implanted dopant profiles during subsequent thermal processing via the mechanism of transient-enhanced diffusion (TED) [1–5]. Many positron works have been undertaken to probe these defects [6–8]. In our recent work [9–11], the defect profiles associated with solid phase epitaxial growth (SPEG) of self-ion implanted silicon were reported. This paper provides additional data on float-zone (fz) Si which indicates that the source of the impurities is not likely to be residual oxygen in the unimplanted crystals.

2. Solid Ar-moderated positron beam

The capability of reducing positron energy from MeV to eV is critical for profiling of defects in films, surfaces, and interfaces since it allows the depth to be controlled by varying positron energy. This reduction in energy is realized by the use of moderators which work because the positron work

* Corresponding author. Tel.: +1-423-574-8955; Fax: +1-423-574-8363; E-mail: yxn@ornl.gov

0169-4332/99/$ - see front matter
PII: S0169-4332(99)00199-3

functions are negative for some materials, such as W and Ni. Most of moderators currently used are based on the negative work functions of positrons. However, other moderators involve positron scattering in large band-gap solids, such as rare-gas solids [12] and possibly SiC [13]. In this work, a solid Ar moderator is described, which is easily prepared and very efficient in producing slow positrons.

The ORNL positron beam, originally developed at Bell Laboratories, consists of a 20 mCi ^{22}Na radioactive source, a solid argon moderator, a ExB filter, and additional beam-guidance equipment. The source emits fast positrons with energy peaking at a few hundred kilo-electron-Volts. These high-energy positrons are moderated by an Ar film, which is prepared by admitting Ar gas into a 4-K cold finger. Slow positrons are driven out of the moderator by biasing the moderator film at 10 V. Two pairs of ExB plates are used to filter the residual high-energy positrons. Positron energy is controlled from 10 eV to 30 keV by applying a negative high voltage on the sample. The slow positron beam is then focused on the sample with a diameter of 7 mm.

The Ar film is generated on the inner wall of a W–Cu cup that is attached to a cold (4 K) source holder, shown in Fig. 1. The ^{22}Na source is deposited in a 7.6 mm diameter spot covered with a 5 μm CuBe foil. The source holder is a cylinder fabricated from W–Cu alloy as well. The cup wall has a parabolic shape with an exit hole of 15.2 mm in diameter. Prior to cooling the cup assembly, the vacuum is normally 5.0×10^{-9} Torr. Then a high impurity (99.9995%) Ar gas is introduced into the vacuum chamber at a pressure of about 5×10^{-5} Torr for approximately one hour. Under these conditions, an Ar film, tens of micrometers, is expected. This thickness is sufficient to stop most of the high-energy positrons. After deposition, the film is annealed at 40 K for a few minutes. Following this annealing process, a crystalline film is expected with increases in the moderation efficiency from 30% to 300%, depending on the vacuum conditions. The counting rate of annihilation gamma rays from the target is about 30,000 counts/s, which determines the positron flux to be 0.9 million positrons per second. The fast-to-slow positron conversion efficiency is about 1.2×10^{-3}, about an order of magnitude higher than that of a tungsten moderator [14].

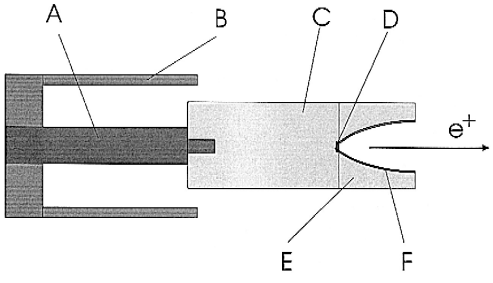

Fig. 1. Setup for solid Ar moderator. A: 4 K colder finger; B: Heat shielding; C: W–Cu source holder; D: 20 mCi ^{22}Na source; E: W–Cu Cup; and F: Ar film.

It is important to note that the positron yield decays as a function of time. This is especially a problem considering that *S* parameter, an experimental parameter sensitive to defects, generally depends on the counting rate. To minimize this problem, purification of Ar gas and maintenance of the high vacuum are helpful. For a pressure lower than 8×10^{-9} Torr, the half-life of the positron intensity is about a week. Since the vacuum is an important issue both during the formation of the Ar film and operation, an ion pump with its pumping speed of 220 l/s was added to the original Bell Labs system to lower the ultimate pressure to 4×10^{-9} Torr for just about two days of baking the system. The original getter furnace used at Bell Labs will be installed for further decreasing impurities in Ar gas. A pile-up eliminator gates the beam off within 100 ns of the detection of a pulse and a beam rate feedback voltage may be used to maintain a constant beam rate.

Data acquisition software was developed for measurements of the Doppler broadening of the annihilation radiation and positronium (Ps) emission from surfaces under various conditions. The software, written in C++ code, produces two windows. The upper window displays the on-line gamma spectrum and contains parameters from an input file that defines channels for the peak region (*S*), the wind region (*W*), and the *ortho*-positronium (*o*-Ps) of annihilation. The input file also gives control parameters for varying positron energy and other optional variables. The software saves the gamma spectra of all positron energies used. The bottom window, which can be made on-line or off-line, plots the *S*, *W*, or *o*-Ps parameters versus positron energy or time.

3. Defect profiling of dual implanted Si

Slow positrons from the previously described setup were used to characterize samples processed using a dual implant method. This method involves both high-energy self implantation at 250°C and sequential low-energy amorphizing implantation of Si, followed by annealing at 600°C and 800°C. Details of this method are described in Refs. [9–11]. Profiles of interstitial defects generated by this method were profiled by Rutherford back scattering (RBS)/channeling measurements [15]. However, there are very few studies on profiling of vacancies associated with this method, even though vacancy defects are known to contribute the diffusion of certain dopants [5]. In this work, Doppler broadening of annihilation radiation and beam positron lifetime spectroscopy have been used to probe vacancy defects.

The samples studied consist of float-zone (fz) Si wafers implanted first by 1.25 MeV Si^+ with a fluence $5 \times 10^{16}/cm^2$ at 250°C and then by 70/140 keV Si^+ to a fluence of $1 \times 10^{15}/cm^2$ at RT. Measurements on similarly treated Cz samples were already discussed in Refs. [9–11]. The low-energy implant fluence was sufficient to produce a continuous amorphous layer at the surface. As shown in Fig. 2, the *S* parameter as a function of depth was measured by varying the positron energy. In the as-implanted sample, the *S* parameters in the region between the surface and the projected range of the high-energy ions (R_p) are remarkably higher than the value (S_b) for perfect Si, suggesting open-volume defects are formed both in the amorphous layer and at substantially deeper depths in the crystal. Following annealing at 600°C for 20 min, sufficient to crystallize the amorphous layer via SPEG, the *S* parameters are dramatically reduced in the SPEG layer. An additional anneal at 800°C for 20 min produces a constant distribution of the low *S* parameters in the entire SPEG layer, as shown by the filled circles in Fig. 2. The *S* parameters in the range of 250–700 nm are much larger than those in the as-implanted sample, presumably due to complexing of the vacancy defects injected by the MeV implant. The large decrease in the *S* parameters in the SPEG layer suggests two possibilities: a reduction in the vacancy concentration and presence of vacancy–impurity complexes, which are known to cause such a reduction in *S* below the bulk value.

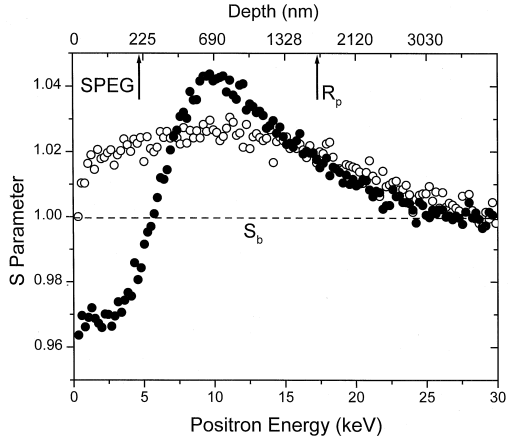

Fig. 2. *S* parameters as a function of positron energy for fz-Si(100) as-implanted (open circles) and post implantation annealing (filled circles). The implant parameters for high-energy implantation are 1.25 MeV with dose of $5 \times 10^{16}/cm^2$ at 250°C. Sequentially, the sample was implanted at low-energy (70/140 keV) Si^+ with a fluence of 1×10^{15} Si^+/cm^2 at room temperature. The annealing at 600°C and 800°C for 20 min was done in a clean Si-only quartz-tube furnace. S_b is the normalized *S* parameter for unimplanted Si. R_p is the projected range of 1.25 MeV Si ions. SPEG is the layer boundary determined by the low-energy Si ions.

To identify specific types of defects, it is necessary to measure both positron lifetime and Doppler broadening spectra. Positron lifetimes were measured at the Electrotechnical Laboratory. A detailed description of the experimental set up is given in Ref. [16]. For the as-implanted sample, positron lifetimes were found to be (307 ± 1 ps) over entire range of implant. This is the same as the divacancy lifetime within experimental errors. Fig. 3 shows the positron lifetimes as a function of positron energy for the dual-energy implanted fz-Si, followed by annealing at 600°C and 800°C for 20 min. Following the SPEG, the lifetime in the regrown layer is unchanged from that prior to annealing. This is very different from the broadening measurements, described above, which show that the *S* parameters are dramatically reduced after the same annealing procedure. The difference between the effects of *S* parameter and positron lifetimes after the post implantation annealing is attributed to the formation of divacancy–impurity complexes. Before annealing, positrons are trapped in the open-volume of the amorphous Si,

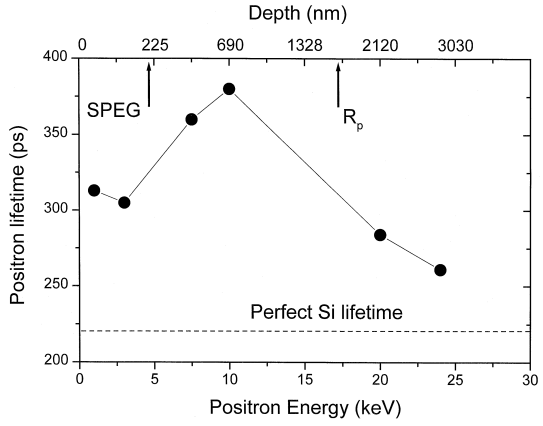

Fig. 3. Primary component positron lifetimes as a function of positron energy for fz-Si(100) implanted and annealed under the same conditions described in Fig. 2. R_p is the projected range of 1.25 MeV Si ions. SPEG is the layer boundary determined by the low-energy Si ions.

which apparently is equivalent in its effect to divacancies in a crystalline lattice. Both the high S parameter and the enhanced lifetime reflect an open-volume structure. During annealing, the open volumes defects, together with the impurities, form divacancy–impurity complexes (V_2–O_n). In this case, positrons remain trapped in V_2 sites of the V_2–O_n complexes which are known to yield a lifetime indistinguishable from the undecorated divacancy lifetime. However, when the trapped positrons annihilate with nearby impurity electrons, the S parameter is expected to be lower than the perfect Si value (S_b). The impurity may originate from oxygen generated by recoil collisions or/and intrinsic boron in the p-type wafer. Under present conditions, there are no specific identification. However, since the data of Figs. 2 and 3 are essentially identical to that of Refs. [9–11], which used Cz-Si, it is not likely that an oxygen impurity would originate from intrinsic residual oxygen in the as-supplied wafers.

As the positron energy increases to 10 keV, which corresponds an average depth of 690 nm, the S parameters are dramatically increased. The lifetime spectrum at this energy has two major components, (83 ± 4)% of 380 ± 5 ps and (16 ± 4)% of 780 ± 23 ps. The 380 ps lifetime indicates larger-size vacancy clusters, close to 5–10 atomic vacancies. Since formation of six atomic vacancies in Si gains larger energy than that for the other vacancies [17], we believe the lifetime and S parameter are attributed to the V_6 vacancy cluster, formed by grouping of the divacancies during annealing. The 780 ps lifetime component suggests the existence of voids near the amorphous–crystalline interface. In this case, both Doppler broadening and positron lifetime measurements suggest there is an aggregation of vacancy clusters.

4. Conclusions

In summary, a solid Ar-moderated positron beam yielding 0.9 million slow positrons per second from a 20 mCi ^{22}Na source, was used to study vacancy defects produced in Si by a dual implant method. Since the apparent formation of vacancies and divacancy–impurity complexes is nearly identical in both float-zone and Czochralski-Si, the source of any impurities is not likely to be intrinsic residual oxygen in the unimplanted Si. Work to identify the chemical environment of the defects using the two-detector Doppler broadening coincidence method is underway.

Acknowledgements

The authors thank S.H. Overbury for his support and helpful discussions. This research was sponsored partly by the ORNL Laboratory Directed Research and Development Program/Seed Money Program and partly by the Division of Materials Science, US-DOE under contract DE-AC05-96OR22464 with Lockheed Martin Energy Research.

References

[1] K.S. Jones, K. Moller, J. Chen, M. PugaLambers, B. Freer, J. Berstein, L. Rubin, J. Appl. Phys. 81 (1997) 6051–6055.
[2] K.S. Jones, L.H. Zhang, V. Krishnamoorthy, M. Law, D.S. Simmons, P. Chi, L. Rubin, R.G. Elliman, Appl. Phys. Lett. 68 (1996) 2672–2674.
[3] H.S. Chao, P.B. Griffin, J.D. Plummer, C.S. Rafferty, Appl. Phys. Lett. 69 (1996) 2113–2115.
[4] H.S. Chao, S.W. Crowder, P.B. Griffin, J.D. Plummer, J. Appl. Phys. 79 (1996) 2352–2363.
[5] S.B. Herner, H.-J. Gossmann, R.T. Tung, Appl. Phys. Lett. 72 (1998) 2289.

[6] P. Asoka-Kumar, K.G. Lynn, D.O. Welch, J. Appl. Phys. 76 (1994) 4935.
[7] N. Hayashi, R. Suzuki, N. Hasegawa, N. Kobayashi, S. Tanigawa, T. Mikado, Phys. Rev. Lett. 70 (1993) 45.
[8] P. Asoka-Kumar, J.-H. Gossmann, F.C. Unterwald, L.C. Feldman, T.C. Leung, H.L. Au, V. Talyanski, B. Nielsen, K.G. Lynn, Phys. Rev. B 48 (1993) 5345.
[9] J. Xu, E.G. Roth, O.W. Holland, A.P. Mills Jr., R. Suzuki, Appl. Phys. Lett. 74 (1999) 997.
[10] O.W. Holland, L. Xie, B. Nelson, D.S. Zhou, J Electron. Mater. 25 (1996) 99.
[11] E.G. Roth, O.W. Holland, V.C. Venezia, B. Nielsen, J. Electon. Mater. 26 (1997) 1349.
[12] A.P. Mills Jr., S.S. Voris Jr., T.S. Andrew, J. Appl. Phys. 76 (1994) 2556.
[13] W. Bauer-Kugelmann, G. Koegel, P. Sperr, W. Triftshaeuser, Mater. Sci. Forum 662 (1997) 255–257.
[14] P. Sferlazzo, S. Berko, K.F. Canter, Phys. Rev. B 32 (1985) 6067.
[15] E.G. Roth, O.W. Holland, A. Meldrum, Proc. 8th International Symp. on Silicon Mater. Sci. and Tech., 1997.
[16] R. Suzuki, Y. Kobayashi, T. Mikado, H. Ohgaki, M. Chiwaki, T. Yamazaki, in: E. Ottewitte, A.H. Weiss (Eds.), AIP Conf. Proc. 303, AIP, New York, 1994, p. 526.
[17] J.L. Hastings, S.K. Estreicher, P.A. Fedders, Phys. Rev. B 56 (1997) 10215.